Talanta 258 (2023) 124389

Contents lists available at ScienceDirect

Talanta

journal homepage: www.elsevier.com/locate/talanta

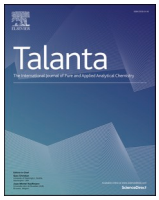

Untargeted metabolomics approach using UHPLC-IMS-QTOF MS for surface body samples to identify low-volatility chemosignals related to maternal care in mice

Leticia Lacalle-Bergeron [a], Rafael Goterris-Cerisuelo [b], Joaquin Beltran [a], Juan Vicente Sancho [a], Cinta Navarro-Moreno [b], Fernando Martinez-Garcia [b], Tania Portolés [a,*]

[a] Environmental and Public Health Analytical Chemistry, Research Institute for Pesticides and Water (IUPA), Universitat Jaume I, Av. Sos Baynat S/N, 12071, Castellón de la Plana, Spain
[b] Laboratory of Functional Neuroanatomy (Unitat Mixta NeuroFun-UV-UJI), Predepartamental Unit of Medicine, Universitat Jaume I, Av. Sos Baynat S/N, 12071, Castellón de la Plana, Spain

ARTICLE INFO

Handling Editor: J. Wang

Keywords:
Untargeted metabolomics
Ion mobility
Chemical signalling
Mouse pheromones
Maternal care
HRMS

ABSTRACT

The present study is focused on the determination of low-volatile chemosignals excreted or secreted by mouse pups in their early days of life involved in maternal care induction in mice adult females. Untargeted metabolomics was employed to differentiate between samples collected with swabs from facial and anogenital area from neonatal mouse pups receiving maternal care (first two weeks of life) and the elder mouse pups in the weaning period (4th week old). The sample extracts were analysed by ultra-high pressure liquid chromatography (UHPLC) coupled to ion mobility separation (IMS) in combination with high resolution mass spectrometry (HRMS). After data processing with Progenesis QI and multivariate statistical analysis, five markers present in the first two weeks of mouse pups life and putatively involved in materno-filial chemical communication were tentatively identified: arginine, urocanic acid, erythro-sphingosine (d17:1), sphingosine (d18:1) and sphinganine. The four-dimensional data and the tools associated to the additional structural descriptor obtained by IMS separation were of great help in the compound identification. The results demonstrated the great potential of UHPLC-IMS-HRMS based untargeted metabolomics to identity putative pheromones in mammals.

1. Introduction

The role of chemicals for intra- and inter-specie communication has been widely demonstrated through the animal kingdom. Many species use true pheromones [1], e.g. chemicals excreted and/or secreted that elicit stereotyped behavioural and/or neuroendocrine-developmental responses in conspecifics [2]. Macrosmatic mammals such as rodents, possess two nasal chemosensory systems for monitoring of chemicals in their environment, including pheromones: the olfactory epithelium (OE), which detects a myriad of volatiles present in the air; and the vomeronasal organ (VNO), which detects compounds with high and low volatility [3]. Screening the response of the VNO of mice to different chemicals revealed that vomeronasal cells also respond to many volatile pheromones as well as to small molecules secreted by predators (carnivores) [4]. The last thirty years of investigation have uncovered many molecules with different physico-chemical properties mediating a wide variety of social interactions including as kin and individual recognition, sexual attraction, dominancy, aggression among others [5]. In addition, several studies have demonstrated a role of chemosensing in the interaction of adult mice with pups. For example, some chemosignals apparently mediate pup killing by sexually-naïve males [6], which seems largely dependent on signalling in cells of the vomeronasal organ [7]. Moreover, induced anosmia results in dramatic changes in the response of females to pups resulting from maternal neglect to systematic pup killing [8,9]. However, it is surprising that no study has been carried out to unveil the chemical cues involved in materno-filial communication, in spite of the crucial role of maternal behaviour in pups survival and development [10].

In our first paper on that issue, it was explored volatile putative pheromones involved in materno-filial communication in mice [11] by comparing the volatolome of neonatal pups, receiving dedicated care by their mothers, with the volatolome of 4-week pups, e.g. the age of

* Corresponding author.
E-mail address: tportole@uji.es (T. Portolés).

https://doi.org/10.1016/j.talanta.2023.124389
Received 18 November 2022; Received in revised form 14 February 2023; Accepted 19 February 2023
Available online 23 February 2023

weaning. In this study, the aim was focused on those molecules with lower volatility present in the body surface of neonatal pups (anogenital and facial regions) that could induce maternal care in mice, and that decrease with age until weaning. To do so, untargeted metabolomic approach was used for screening metabolites, with the aim to identify those biomarkers which can act as pheromones. This comprehensive methodology aims to differentiate between samples coming from an organism that has suffered changes in their metabolite fingerprinting in response to internal (genetics, disease, growth …) or external (environmental, diet …) perturbations [12,13]. As our objective was to focus on low-volatile compounds excreted or secreted by mouse pups, reversed phase liquid chromatography (RP-LC) was the technique of choice for the separation of medium to non-polar compounds that can constitute some of the released pheromones. The evolution of untargeted metabolomics has been possible thanks to the implementation of powerful statistical tools such as multivariate statistical analysis [14], as well as the great improvement in analytical instrumentation [15]. In particular, ion mobility mass spectrometry (IMS) introduction to the conventional liquid chromatography coupled to high resolution mass spectrometry (LC-HRMS) has an emerging role in untargeted metabolomics in the generation of multidimension data to support metabolites identification [16]. LC-IMS-HRMS combination provides an extra separation dimension through the drift time (DT), later converted into collisional cross section value (CCS, $Å^2$), to the conventional three-dimensional data formed by retention time (Rt), accurate mass (m/z) and intensity from LC-HRMS. This additional molecular descriptor is dependent on the individual size, shape and charge of a molecule, and therefore, it can be transversal between instruments regardless of the chromatographic technique employed [17]. In fact, the CCS value is being added to the compound databases together with the spectral information; and various CCS prediction tools have been developed to help in the compound identification process [18,19]. Therefore, in this work an untargeted metabolomic approach in combination with ultra-high pressure liquid chromatography (UHPLC)-IMS-HRMS was applied to samples collected from facial and anogenital area of mouse pups, in order to identify putative chemosignals with low volatility involved in the maternal care induction, not covered in the first part of the study. In addition, the contributions of IMS and its associated tools to the identification process are explored.

2. Materials and methods

2.1. Chemicals and reagents

Methanol LC-MS grade was purchased from Scharlab (Barcelona, Spain), as well as formic acid eluent additive for LC-MS. To obtain HPLC-grade water a Milli-Q water purification system (Millipore Ltd., Bedford, MA, USA) was employed. Leucine-enkephaline HPLC-grade (mass axis calibration) was purchased from Sigma-Aldrich (Saint Louis, MO, USA).

2.2. Animals, experimental design and sampling

To perform the study, a total of $n = 4$ mouse female (CD1 strain, 10-week-old) (Janvier Labs, France) were employed. Animals were treated throughout according to the European Union Council Directive of June 3rd, 2010 (6106/1/10 REV1) and the study was approved by the Committee of Ethics on Animal Experimentation of the Jaume I University of Castellón, where the experiments were carried out and, ultimately, by the Valencian *Conselleria d'Agricultura Medi Ambient, Canvi Climàtic i Desenvolupament Rural* (code 2019/VSC/PEA/0049).

After mating with an adult male, the pregnancy was carefully controlled following the conditions extensively described in Lacalle-Bergeron et al., 2021 [11]. This second study was carried out simultaneously to the one referred in our previous article and used the same animals.

Two of the females delivered 17 days before the other two as planned, in order to process in parallel pups of different ages. In this way, the first day of experimentation, right after the volatolome extraction for our previous study [11], the surface of the body pheromones was sampled simultaneously in neonatal pups (4-day old) and pups at the age of weaning (21 days-old), by gently rubbing their anogenital region with a cotton swab for 1 min, and then the orofacial region (eyes, nose, mouth) with another cotton swab. This sampling procedure was performed for four consecutive days per week, thus obtaining samples from pups of 4-to-7-days old (1st week pups) in parallel to 21-to-24-days old (4th week pups). The following week, the younger pups were sampled again, thus obtaining samples from 10-to-13-days old pups (2nd week pups).

2.3. Extraction of low-volatile putative pheromones

Three swabs coming from the same body area of 3 pups selected randomly from the same litter (siblings, with independence of the sex) were soaked together in 1500 μL of acetone and further extracted in a thermostatic water bath at 25 °C with ultrasound assistance for 20 min (Fig. 1). Then, the organic solvent was evaporated to dryness at 35 °C under a gentle stream of nitrogen, to finally reconstitute the residue in 150 μL of methanol for instrumental analysis. In total, four samples per day and per area were obtained, and 4 days were studied per week (Table 1). Each day of analysis, blank extracts were performed following the same procedure with three clean swabs. From each sample extract, 50 μL were aliquoted to be pooled as a quality control sample (QC), which was injected at the beginning of the sample batch for chromatographic column conditioning and every 10 samples to ensure the stability and repeatability of the system.

2.4. Instrumentation

Ultra-high performance liquid chromatography (UHPLC) with ACQUITY UHPLC I-Class system (Waters, Milford, MA, USA) was coupled to a VION® IMS QTof (Waters, Manchester, UK), ion mobility hybrid quadrupole time-of-flight (IMS-QTOF) high resolution mass spectrometer (UHPLC-IMS-HRMS) using electrospray interface operating in positive ionisation mode (ESI+). Equipment control, data acquisition and processing were performed using UNIFI software (V.1.9.2, Waters, Manchester, UK).

The chromatographic separation employed was reversed phase liquid chromatography (RPLC) using a CORTECS® C18 fused-core 2.7 μm particle size analytical column 100 × 2.1 mm (Waters). The flow rate was set at 0.3 mL/min, column oven at 40 °C and 1 μL sample injection volume was selected. The mobile phases employed were A = H_2O and B = methanol, both with 0.01% formic acid. The gradient changed from 10% B at t = 0 min to 90% B at t = 14 min, holding it for 2 min, and at t = 16.01 min B decreased to 10% and held for 2 min; total run time 18 min.

Regarding the HRMS analyser, the capillary voltage was set at 0.7 kV in ESI + ionisation mode. Nitrogen was used as desolvation gas, nebulising gas, mobility gas and collision gas. Source temperature was set to 120 °C and desolvation gas to 550 °C with a flow rate of 1000 L/h. The HRMS analyser operated in MS^E acquisition mode combined with ion mobility separation ($HDMS^E$). As normal MS^E acquisition mode, it is a type of data independent acquisition (DIA) analysis where two functions are acquired sequentially: low energy function (LE), with a fixed collision energy at 6 eV, and high energy function (HE) with a ramp of collision energy from 28 to 56 eV. Both acquisitions were performed from 50 to 1000 Da and at 0.3 s scan time.

"Major Mix IMS/T of Calibration kit" (Waters) infused at 20 μL/min flow rate was used for calibration of mass axis and drift time. For automated accurate mass correction, 100 ppb Leucine-Enkephalin acetonitrile:H_2O (50:50, *v/v*) at 0.01% formic acid solution was infused at 20 μL/min into the system through the lock-spray needle and measured every 5 min with 0.3 s scan time during the sample injection

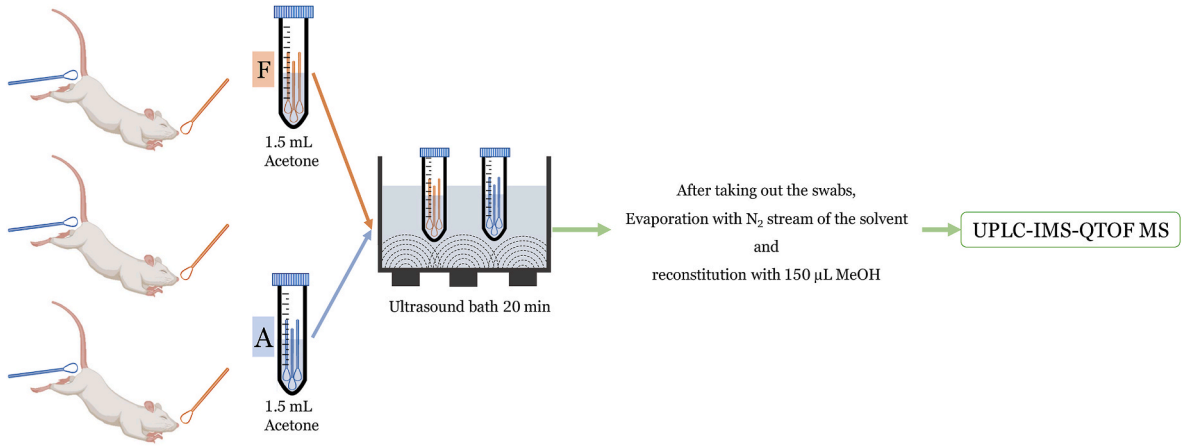

Fig. 1. Experimental design used for alive mice pup low-volatility putative pheromones collection. Swabs for facial area sampling are coloured in orange and those for the anogenital area in blue. Three swabs from different mice pups but from the same zone (F = facial or A = anogenital) were extracted together.

Table 1
Mice pup characteristics for each experiment day.

Experiment	Nº of replicates	Nº of mice pups per replicate	Postnatal week	Postnatal day	Mean mice pup weight
1	4	3[a]	1	4	2.6 ± 0.4 g (*n* = 24)
2	4	3[a]	1	5	3.0 ± 0.4 g (*n* = 24)
3	4	3[a]	1	6	3.4 ± 0.5 g (*n* = 24)
4	4	3[a]	1	7	3.9 ± 0.5 g (*n* = 24)
5	4	3[b]	2	10	5.2 ± 0.8 g (*n* = 18)
6	4	3[b]	2	11	5.6 ± 0.7 g (*n* = 18)
7	4	3[b]	2	12	5.9 ± 0.7 g (*n* = 18)
8	4	3[b]	2	13	6.2 ± 0.8 g (*n* = 18)
9	4	3[c]	4	21	12.5 ± 0.8 g (*n* = 9)
10	4	3[c]	4	22	13.3 ± 0.8 g (*n* = 9)
11	4	3[c]	4	23	14.5 ± 0.8 g (*n* = 9)
12	4	3[c]	4	24	15.6 ± 0.9 g (*n* = 9)

[a] 3 mice selected aleatorily from the 8 mice pups of each replicate for the volatile extraction explained in Lacalle-Bergeron et al., 2021.
[b] 3 mice selected aleatorily from the 6 mice pups of each replicate for the volatile extraction explained in Lacalle-Bergeron et al., 2021.
[c] 3 mice selected aleatorily selected for the volatile extraction explained in Lacalle-Bergeron et al., 2021 where the same for this second experiment.

(ensuring a measurement at the beginning and at the end of each run), monitoring the protonated molecule *m/z* 556.27658.

2.5. Data processing and statistical analysis

Raw data from VION instrument (*.uep*, UNIFI, Waters) were imported into Progenesis QI (v3.0, NonLinear Dynamics, Waters, UK) for data processing. Progenesis QI software automatically performs 4D peak picking (based on *m/z*, retention time, drift time and intensity); retention time alignment (with QC samples as references, except the first 9 QC injection employed for column stabilisation purposes); and response normalisation. Peak picking conditions were set as follows: all runs, sensitivity automatic (level 3), minimum chromatographic peak width 0.1 min and retention time limits from 0.4 to 17 min from the total run time of 18 min. The deconvolution was applied attending to the selected adducts and ion forms for positive ESI+: $[M+H]^+$, $[M+Na]^+$, $[M+K]^+$, $[M\text{-}H_2O+H]^+$, $[2\,M+H]^+$ and $[2\,M+Na]^+$. The samples were divided in groups in the "Experimental Design Setup" section of the software according to the experiment and statistical comparison, starting by a basic classification depending on the area (facial or anogenital) and the week of life (week 1, week 2 or week 4), following the "Between -subject Design" comparison (samples from a given subject appear in only one condition). One-way ANOVA calculation followed by a false discovery rate (FDR) was performed to test differences among the groups, setting the level of statistical significance at 95% (*p-value* <0.05).

The main work of statistical analysis was performed with EZinfo (v3.03, Umetrics, Sweden), focusing on multivariate statistical analysis. After pareto-scaling of the data, the process started by unsupervised Principal Component Analysis (PCA) in order to check the correct acquisition of the samples based on the grouping of the QC replicates in the centre of the plot; and detect possible outliers. Then, Partial Least Square-Discriminant Analysis (PLS-DA) to maximise the separation between the pre-determined groups and the validation of the model was performed by leaving-1/7-out cross-validation approach. Finally, Orthogonal PLS-DA (OPLS-DA) was carried out to highlight the most significant markers between the faced groups (threshold *p(corr)* $\geq |0.6|$ and *p* [1] *loading* $\geq |0.1|$).

3. Results and discusion

3.1. Experimental set up for low volatile putative pheromone obtention

As explained in the previous research article [11], the procedure employed did not interfere with pup's growth and comfort (pups gained weight according to the standards) (Table 1). The sampling from pups was carried out quickly and accurately by the personnel accredited in

animal handling so that the process was as stress-free as possible for the animals under study. The pups were returned after the sampling to its mother and kept under the appropriate and controlled conditions for its development until the next day of sampling.

Based on the premise that some of the compounds with a putative role as pheromones inducing maternal care could not be very volatile, this second experiment was focused on low volatile compounds of exocrine glands secreting an aqueous medium, such as saliva or sweat, or excreted in urine. In both cases, these compounds are expected to be rather polar compounds. Less polar compounds, which could be significant for chemical communication, could also be secreted by sebaceous glands.

The starting hypothesis was that mouse pup pheromones are secreted/excreted during the first days of life, when dams exhibit dedicated pup care, but their release decreases with age until weaning.

Besides the molecules that are excreted in urine/faeces, most chemosignals must derive from secretions of exocrine glands: salivary, lacrimal and other glands located in the chin perineal and genital areas. This is the reason why sampling was focused on the anogenital and facial areas. To extract them from the skin, swabs were rubbed around each area during 1 min and samples coming from each of them were treated separately. Afterwards, the extraction of the collected molecules with the swabs was carried out in acetone. The choice of the solvent was based on its compatibility with molecules in medium range of polarity and the ruling out of those too large to be covered in a metabolomic study, such as proteins.

As the pheromones should be released in a very similar way in all pups of the same age, and regardless the sex, 3 mouse pups of the same day of age were randomly chosen for each sample extraction. The collected sample from each area of those 3 pups were extracted in the same 1500 μL of acetone to increase the concentration (Fig. 1).

RPLC with a C18 column was selected due to well-known behaviour, good robustness and its ability to cover a wide range of compounds. Due to the high sensitivity of the instrument employed and the small injection volume required (1 μL), no additional sample treatment steps were necessary, such as evaporation and reconstitution in more compatible solvent for the chromatography. As it is a common practice in chromatography-MS-based metabolomics, the quality of the results and the analytical process were monitored by means of injection of mechanic replicates (every 10 samples) of quality control sample (QC sample, a homogeneous pool of all treated samples) during the chromatographic run. Moreover, it is highly recommended to perform the sample treatment and the acquisition in a randomised way. Although this could not be possible in the sample treatment, as the extraction was performed as the mouse pups grew up, it was applied for the UHPLC-IMS-HRMS acquisition of the data, assuring that the possible instrumental drift during the sequence did not affect to a group more than others and minimising the bias.

3.2. Data processing and statistical analysis

The data set acquired with UNIFI software (Waters, UK) was exported to *.*uep* format (UNIFI export package). To the best of our knowledge, only Progenesis QI (nonlinear Dynamics, UK) program is able to process and interpret four-dimensional data (Rt, *m/z*, intensity and DT) for -omics purposes. After the data import, Progenesis QI performs 4D peak picking, followed by retention time alignment and finally normalisation. For the retention time alignment one sample between the QC replicates was selected as reference (except the first 9 QCs samples injected at the beginning of the chromatographic run for column stabilisation). All samples had a high and very good alignment (all above 90%) and normalisation method for the aligned data was "normalisation to all compounds". The resulting data matrix consisted in the detection of 6094 signals that Progenesis QI assigned to a total of 5454 features, due to the automatic deconvolution performed with the specified adducts selected in the setting of the peak picking. Therefore, for those features where more than one adduct was detected the program will annotate them as *xx.xx_yyy.yyyy*n (*xx.xx* being the retention time in minutes and *yyy.yyyy* the exact neutral mass calculated when more than one adduct ion is found for the same compound); and for single ions *xx.xx_zzz.zzzzzm/z*, *zzz.zzzz* being the accurate mass. The 5454 data set was reduced to 3647 features after the removal of all features with poor stability in the QCs samples, keeping all features with a relative standard deviation (% RDS) below the 30% within the QCs.

An exploratory visualization of the data was performed by unsupervised multivariate analysis PCA in order to observe trends, inherent grouping of the data and possible outliers. As QC is considered as an "average" sample (constituted by a pool of all analysed samples), and it is injected after every 10 samples ($n = 12$ replicates), the clustering in the centre of the PCA score demonstrated the correct acquisition of the run, determining that the inherent differentiation between the samples does not come from an instrumental drift during the acquisition of the data. QC samples grouping near to the centre can be observed in Fig. S1, PCA score of component 1 vs component 2, proving the proper performance of the analytical system. Nevertheless, no inherent differentiation was observed between the groups of samples. Only a slight separation of blank samples can be noticed in the upper left quadrant. Twelve principal components were necessary to explain the 88% of the total variance. The blanks data were removed from the subsequent statistical analysis, although they were consulted later to validate the features highlighted in the statistics as markers by checking their absence in these samples, demonstrating that they did not come from the swabs employed or any other factor during the experimental procedure.

Then the statistical analysis was focused on the differentiation of the samples by the age of mice pup, analysing samples coming from facial and anogenital separately. Taking into account the information of the volatolome separation from the first part of the study, univariate statistical analysis was applied obtaining 338 and 912 statistically significant features for the differentiation by week of the samples in the facial area and in the anogenital area, respectively. From these reduced data matrices, a second PCA was applied to interrogate the data (Fig. S2 A and **B**). Four components were enough to explain the 83% of the variance for the differentiation by the compounds collected from the facial area and eight components for the 87% of the variance explained for the anogenital area. Colouring the samples according to the week of life in these two PCA, a separation by age can be observed, the samples coming from the aged pups (week 4) are clearly differentiated from the samples coming from the younger ones. A slight differentiation of samples from the first and second week of life might be appreciated in the samples coming from the facial area by the 2nd component (Fig. S2A) that it is not observed for the anogenital region (Fig. S2B). Some samples were taken as possible outliers, especially in the PCA from anogenital samples, and they were studied in the following analysis before considering eliminating any of them from the statistics.

Subsequently, PLS-DA was applied to both data sets, attempting to target a grouping by week of life in this supervised multivariate statistical analysis. The PLS-DA score plots facing the first two latent variables are shown in Fig. 2A and **B**, where classification of pups by weeks is appreciated. For PLS-DA based on the compounds extracted from the facial region it was obtained a 64% of the variance explained and a 52% of the variance predicted with three latent variables. The PLS-DA from anogenital area obtained a variance explained of 80% and a predicted of 58% with five latent variables. Although these results in the variance might seem lower than desirable and close to the accepted limit of 50% for variance explained and 40% for predicted for biological models [20], this is mainly due to the difficulty in separating the groups of the first two weeks. However, a clear differentiation of the groups of samples that come from the oldest pups can be observed along the first latent variable of both PLS-DAs, the one that explains the greater differentiation of the model (52.3% for facial area and 36.2% in anogenital area).

Following the objective on finding molecules with higher presence in the first weeks, a binary differentiation was attempted with OPLS-DA,

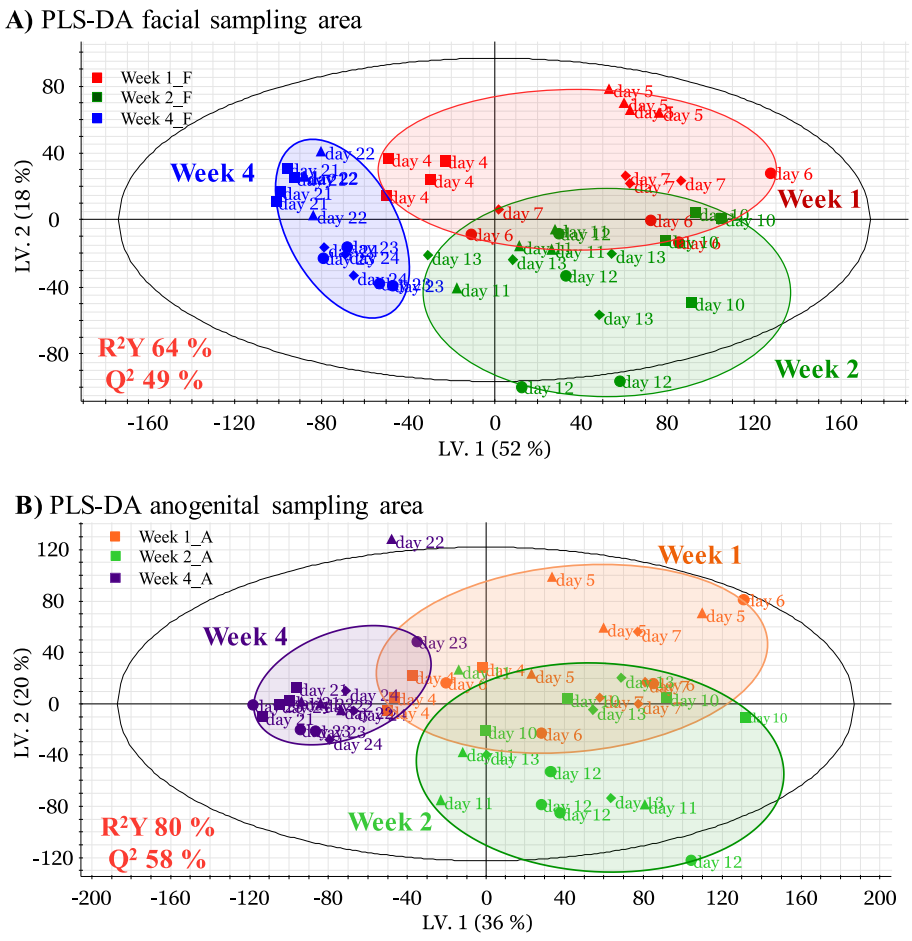

Fig. 2. PLS-DA score plot latent variable 1 vs latent variable 2 of from **A**) Facial and **B**) Anogenital areas coloured by week: 1st week facial area (Week 1_F■), 2nd week facial area (Week 2_F■), and 4th week facial area (Week 4_F■); and for anogenital area 1st week (Week 1_A■), 2nd week (Week 2_A■) and 4th week (Week 4_A■).The shape of the marker changed according to the day of the week (1st day of the week □, 2nd day Δ, 3rd day ○ and 4th day ◊)). Being R^2Y is coefficient for variance explained and Q^2 is coefficient for variance predicted, the following results were obtained: R^2Y = 64% and Q^2 = 49% for facial sampling area and R^2Y = 80% and Q^2 = 58% for anogenital sampling area.

starting by week 1 vs week 4 expecting that this facing would be the most significant; and followed by week 2 vs week 4 differentiation, obtaining in all of them a variance explained above the 80% and above the 70% for the variance predicted (Table 2). The S-plots from the OPLS-DA allowed an easiest selection of putative markers in each binary differentiation. The most differentiating features are those with a *p(corr)* closer to 1 or -1 (y-axis of the S-Plot), and with higher intensity the ones with a *p* [1] *loading* closer to 1 or -1 (x-axis of the S-Plot). All features with a *p(corr)* higher than |0.6| and a *p* [1] *loading* above |0.1| were selected as putative markers (Fig. 3 and S3). A total of 17, 14, 12 and 16 features were highlighted in the corresponding S-Plots of facial sampling area week 1 vs week 4 and week 2 vs week 4 and anogenital sampling area week 1 vs week 4 and week 2 vs week 4, respectively. In sum, a total of 34 features highlighted as putative markers, since the features with higher abundance for week 1 used to be the same as the ones more abundant in week 2, hence the little differentiation in the PLS-DA of these two groups. In fact, the 1st week vs 2nd week facing in the OPLS-DA was also applied with poor statistical results. Since the objective of the study was not to confront these two groups, no further investigation was made of said separation.

Moreover, most of the highlighted markers in the facial sampling area were the same as in anogenital area. One reason could be the presence of similar glands in both regions, as sweat and sebaceous glands. On the other hand, the continuous licking of pups by dams could cause that the compound released by one of the areas ended up in the other one. Before starting with the elucidation process, it was studied the presence of these features in the blank samples, thus discarding 23 out of 34 markers since their signals in these samples were relevant enough to question their validity as markers. The fact that certain features with relevant presence in the blanks have passed the statistical filters could be due to an unpredictable lack of homogeneity between the swabs employed for sampling. All remaining features were markers of the 1st and the 2nd week when they were faced to the 4th week. Nevertheless, the list can be further reduced as some type of adducts were not set in the peak picking processing, and therefore not clustered as a single compound; or because of the presence of some in-source fragments (formed prior to the IMS, and therefore with different DT) detected as a different feature.

Table 2
Parameters of the OPLS-DA models.

Statistical model/ Characteristics	OPLS-DA model diagnostics			
	Facial sampling area		Anogenital sampling area	
	Week 1 vs Week 4	Week 2 vs Week 4	Week 1 vs Week 4	Week 2 vs Week 4
	n = 16 vs 16	*n* = 16 vs 16	*n* = 16 vs 16	*n* = 16 vs 16
Components	2	3	4	4
Goodness-of-fit parameter - R^2X	69%	74%	74%	77%
Variance explained – R^2Y (cum)	80%	92%	94%	96%
Variance predicted – Q^2 (cum)	71%	86%	83%	88%

R^2 - fit how model fits the data and Q^2 – predictive ability, by seven-round internal cross-validation as default option of EZinfo software (Umetrics, Sweden).

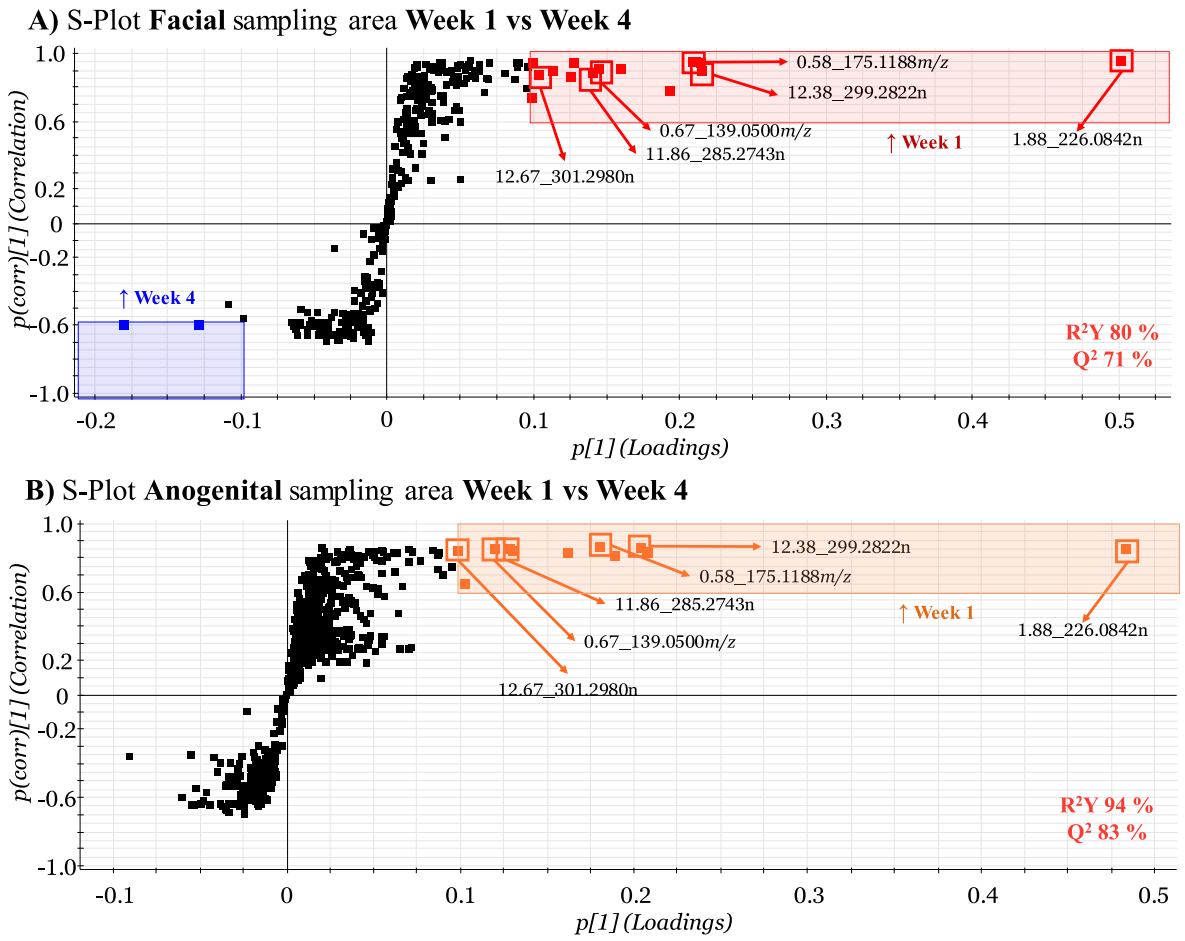

Fig. 3. S-Plots from OPLS-DA score plots and from A) Facial sampling area Week 1 vs Week 4 and B) Week 1 vs Week 4. Being $R^2Y$and Q^2 coefficients are founded in Table 2. The coloured features in the S-plots were the ones selected as putative markers, their colours depend on the week where they are highlighted as markers.

3.3. Elucidation process

The remaining 19 putative markers were studied in order to obtain a tentative identification. To do so, features were annotated with Progenesis QI identification tool based on the deconvoluted $HDMS^E$ spectra and CCS data by search and comparison with exact mass, MS/MS and CCS (if available) information in compound and spectral databases (Metlin, HMDB, *Metabolic Profiling CCS library* for Progenesis QI, LipidBlast …). Moreover, the experimental information about the parent ion, fragmentation spectra and CCS were carefully reviewed from UNIFI raw data. The identification level of each marker (Table 3) was set according the criteria of our laboratory based on Celma et al. (2020) classification [21]. In Table 3 the experimental and statistical data for each tentatively identified marker are recorded.

Markers 1 and 2 received urocanic acid and arginine as identifications, respectively, by match MS/MS and CCS data with available libraries (*Metabolic Profiling CCS library* for Progenesis QI constituted of experimental data for fragmentation and CCS measured in Waters TWIMS instruments). These two markers had a *p(corr)* higher than 0.85 for week 1 and 2 in both facial sampling area and anogenital (see Table 3). As an example, the elucidation process for marker 1 is explained hereafter. Progenesis QI performed a deconvolution of the spectra from LE (6 eV collision energy) and HE (ramp of collision energy from 28 to 56 eV) and compared the results and CCS data with the available compound/spectral databases. Even the best annotation provided by Progenesis QI (defined by the identification score of each candidate) was carefully reviewed with raw data. Fig. 4 shows the obtained UNIFI raw data for Marker 1 (0.67_139.0500 *m/z*, CCS 131.15 $Å^2$), including the extracted ion chromatograms and $HDMS^E$ spectra. As IMS takes place prior to the collision cell, the product ions from fragmentation are linked to their parent ion by the DT of the last one. For this reason, it is possible to obtain cleaner spectra without the interference in the LE spectra of co-eluting ions and their fragments in the HE spectra. Fig. 4B and **C** shows the LE and HE spectra not only aligned by the retention time (0.67 ± 0.04 min), as it is usual in conventional LC-HRMS, but also by the DT (3.09 ± 0.21 ms), obtaining cleaner spectra for both energy functions. As part of the verification, the extracted ion chromatograms of both fragments were obtained from the HE function (Fig. 4A) to verify that the peak shape is similar to the one from parent ion. Both fragments are almost the only fragments found in the experimental spectra of databases. All this process allowed the selection of Urocanic acid as tentative identification among the other candidates (e.g. 4-nitroaniline or methyl-2-pyrimidine carboxylate, isomeric compounds with different fragmentation patterns). Moreover, there was a match with a delta error of +1.35% (maximum tolerance 2%) with the available experimental CCS library for Progenesis QI, increasing the confidence in the tentative identification. This marker finally reached a level 1 of identification by comparison of the experimental data with the reference standard.

Marker 2 (0.58_175.1188 *m/z*, CCS 136.03 $Å^2$) elucidation was carried out in similar way to the process explained, ending in the tentative identification as arginine. The match with the CCS library obtained a delta error of +0.17%. In this case, an in-source fragment (due to an ammonia neutral loss from the amino group) was also highlighted as marker (0.58_158.0928 *m/z*, CCS 132.20 $Å^2$). Additionally, this compound was also detected with a second injection of one sample

Table 3
Compound list obtained from the untargeted metabolomic approach: identification and statistical parameters.

No.	Identification level[a]	Compound	Elemental composition	*p (corr)*	Marker of	Feature name	Rt (min)	Protonated molecule *m/z*	Mass error (mDa/ppm)	Experimental CCS (Å^2) protonated molecule *m/z*	CCS delta error (%)	Adducts detected
1	1	Urocanic acid	$C_6H_6N_2O_2$	0.91	W1, Facial W1 vs W4	0.67_139.0500 *m/z*	0.67	139.0500	−0.2/-1.4	131.15	+1.70 %[b]	$[M+H]^+$
				0.90	W2, Facial W2 vs W4							
				0.88	W1, Anogenital W1 vs W4							
				0.85	W2, Anogenital W2 vs W4							
				0.61	W2, Anogenital W1 vs W2							
2	1	Arginine	$C_6H_{14}N_4O_2$	0.95	W1, Facial W1 vs W4	0.58_175.1188 *m/z*	0.58	175.1188	−0.2/-1.1	136.03	+0.07 %[b]	$[M+H]^+$
				0.92	W2, Facial W2 vs W4							
				0.90	W1, Anogenital W1 vs W4							
				0.89	W2, Anogenital W2 vs W4							
3	1	Sphingosine (d18:1)	$C_{18}H_{37}NO_2$	0.90	W1, Facial W1 vs W4	12.38_299.2822n	12.38	300.2901	−0.2/-0.5	195.35	−1.0 %[b]	$[M+H]^+$ $[M-H_2O+H]^+$
				0.70	W2, Facial W2 vs W4							
				0.89	W1, Anogenital W1 vs W4							
				0.79	W2, Anogenital W2 vs W4							
4	1	Sphinganine (d18:0)	$C_{18}H_{39}NO_2$	0.87	W1, Facial W1 vs W4	12.67_301.2980n	12.67	302.3053	−0.1/-0.3	197.60	−1.27 %[b]	$[M+H]^+$ $[M-H_2O+H]^+$
				0.87	W1, Anogenital W1 vs W4							
				0.76	W2, Anogenital W2 vs W4							
5	1	Sphingosine (d17:1)	$C_{17}H_{35}NO_2$	0.88	W1, Facial W1 vs W4	11.86_285.2743n	11.86	286.2743	−0.3/+1.0	192.29	−1.58 %[b]	$[M+H]^+$ $[M-H_2O+H]^+$
				0.89	W1, Anogenital W1 vs W4							
				0.75	W2, Anogenital W2 vs W4							
6	4	Unknown	$C_{11}H_{14}O_5$	0.95	W1, Facial W1 vs W4	1.88_226.0842n	1.88	227.0916	−0.4/+1.5	145.21		$[M+H]^+$ $[M+Na]^+$ $[2\,M+Na]^+$
				0.91	W2, Facial W2 vs W4							
				0.87	W1, Anogenital W1 vs W4							
				0.86	W2, Anogenital W2 vs W4							

c CCS delta error (%) by comparison with the predicted CCS for protonated molecule obtained by LipidCCS prediction tool developed by Zhou et al. (2017).
[a] Identification level according to Celma et al. (2020).
[b] CCS delta error (%) by comparison with the experimental CCS from the injection of its reference standard.

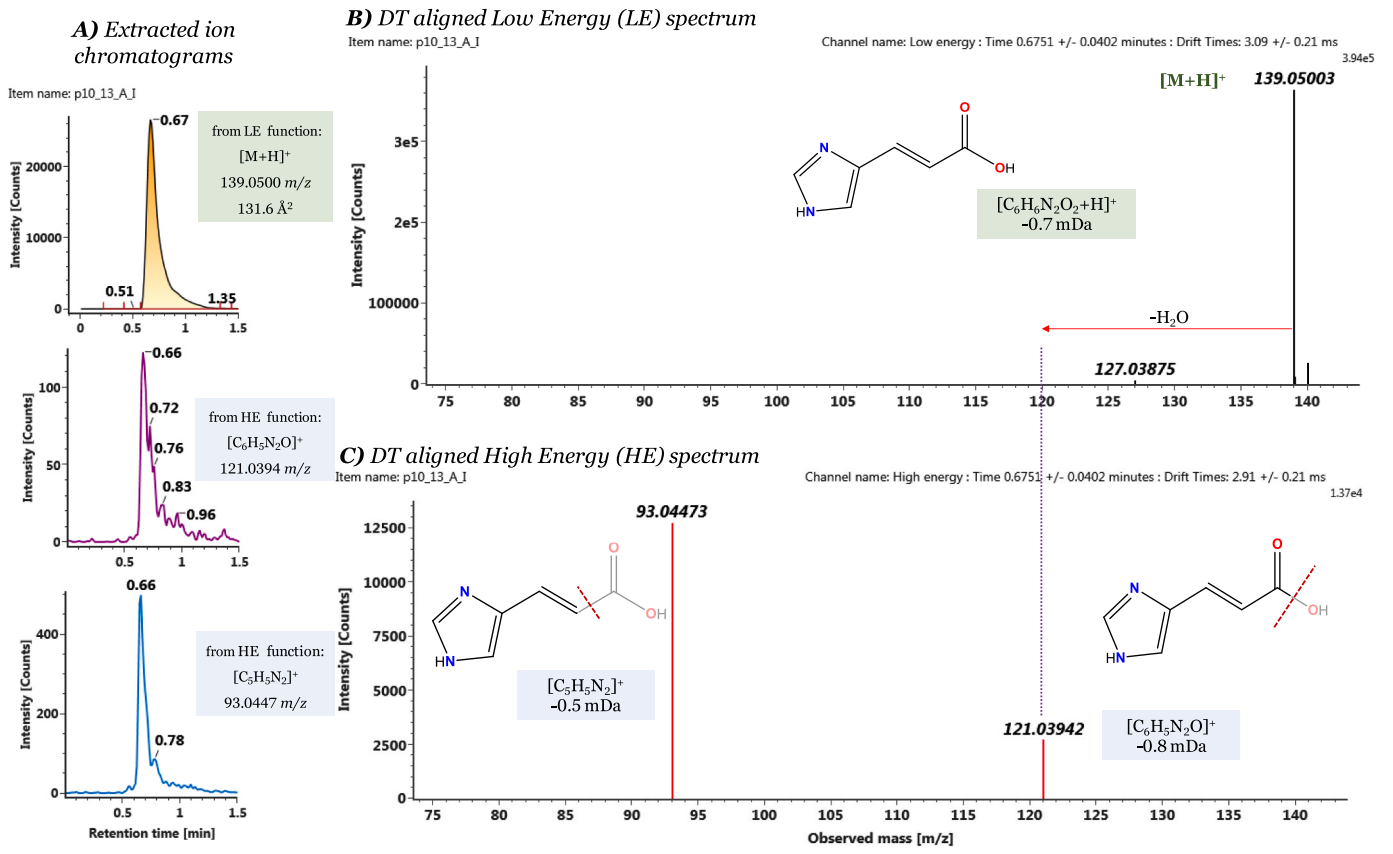

Fig. 4. Elucidation of Marker 1 Urocanic acid based on the chromatograms and HDMS^E spectra: **A**) Extracted ion chromatogram from the LE for the parent ion and HE for both fragments along with their experimental *m/z* and CCS, **B**) DT aligned LE spectrum, **C**) DT aligned HE spectrum. A structure fragmentation is proposed.

from each sampling area in negative ionisation mode ([M − H]$^-$ = 173.1043 *m/z*, retention time 0.59 min, 135.29 Å^2) following the same chromatographic conditions, increasing the identity confidence as arginine is a compound also susceptible to be ionised under negative ESI mode: The identity of marker 2 was also finally confirmed with the reference standard.

The elucidation process of markers 3 (11.86_285.2743n, CCS 192.29 Å^2), 4 (12.38_299.2822n, CCS 195.35 Å^2), and 5 (12.67_301.2980n, CCS 197.60 Å^2) was the same as explained above. These three markers were tentatively identified as three free-sphingoid bases, compounds that are formed by a long aliphatic chain with a polar 2-amino-1,3-diol terminus (Fig. S4). All three showed a similar fragmentation pattern, conformed by 3 fragments due to common neutral loses –H_2O (loss of one hydroxyl group), −2 x H_2O (loss both hydroxyl groups) and the water loss with consecutive formaldehyde (HCHO) loss. Marker 3 was tentatively identified as Sphingosine (d18:1) and marker 4 as Sphinganine (d18:0). For marker 5, three isomeric candidates were possible: erythro-sphingosine (d17:1), (4,14-methy-d16:1) sphingosine and (4,15-methy-d16:1) sphingosine (Fig. S4). The in-source loss of H_2O ([M-H_2O + H]+) (set as possible ion in the Progenesis PQI deconvolution settings) was present in all three markers, being the predominant ion in the LE spectra in the case of unsaturated markers 3 and 5. For sphinganine (d18:0) (marker 4) a delta CCS error of +0.40% was obtained with the match in experimental library. In the other two (3 and 5), CCS values were predicted using a tool optimised for lipids, LipidCCS [22]. This model was optimised by measuring CCS of a large set of lipids with Drift Tube Ion Mobility instruments (DTIMS), with median relative errors (MRE) of ~1%. They ensured that similar error can be obtained with Travelling Wave Ion Mobility instruments (TWIMS) as VION® when lipid CCS calibrants are employed. Recent studies have also demonstrated that CCS values obtained with DTIMS or TWIMS technology can be comparable, and therefore the prediction tools [23,24]. Even so, this tool allowed to rule out (4,14-methy-d16:1)-sphingosine and (4,15-methy-d16:1)-sphingosine as candidates, since delta CCS error found exceeded −30%, and select Erythro-sphingosine (d17:1) as tentative identification for marker 4. Sphingosine (d18:1) (marker 3) obtained a delta CCS error of −1.1%. Finally, the identity for the 3 free-sphingoid bases was confirmed and they reach the level 1 of identification [21].

Regarding marker 6 (1.88_226.0842n, CCS 145.21 Å^2), it is one of the most significative markers for the first two weeks of life due to its high *p(corr)* and high intensity in all the OPLS-DA facings (Fig. 3 and S3). In addition to the protonated and sodium adducts, sodiated dimer was also detected. Moreover, 4 features highlighted in the statistical analysis were associated to this compound as in-source fragments (1.87_125.0595 *m/z*, CCS 123.65 Å^2; 1.87_170.0569 *m/z*, CCS 129.58 Å^2; 1.88_153.0544 *m/z*, CCS 125.91 Å^2; and 1.88_167.0701 *m/z*; CCS 145.21 Å^2). The HDMS^E spectra are shown in Fig. 5, where some of the highlighted in-source fragments can be observed in the DT aligned LE spectra. The fact that these fragments highlighted as markers, with different CCS and therefore DT from the parent molecule, can also be seen in the aligned LE spectra, shows the easy fragmentation with little energy of these molecule not only prior to the IMS (giving different CCS) but also post IMS in the collision cell with 6 eV (associated to the CCS of the parent ion). Consequently, all of these fragments are also observed in the aligned HE spectrum, along with many other fragments. In fact, this molecule presents a very rich fragmentation spectrum, which together with the isotopic pattern and the adducts found, renders a definitive molecular formula as $C_{11}H_{14}O_5$ (+0.3 ppm error). Many similar compounds obtained (Fig. S5) an acceptable match when comparing the DT aligned HE spectrum with the compound/spectral libraries (Metlin, HMDS, *Metabolic Profiling CCS Library* from Progenesis QI, among others libraries from ChemSpider specialised in metabolites). Above all, a definitive identification could not be given to this compound. On one hand, some fragments were present in the spectra of several candidates

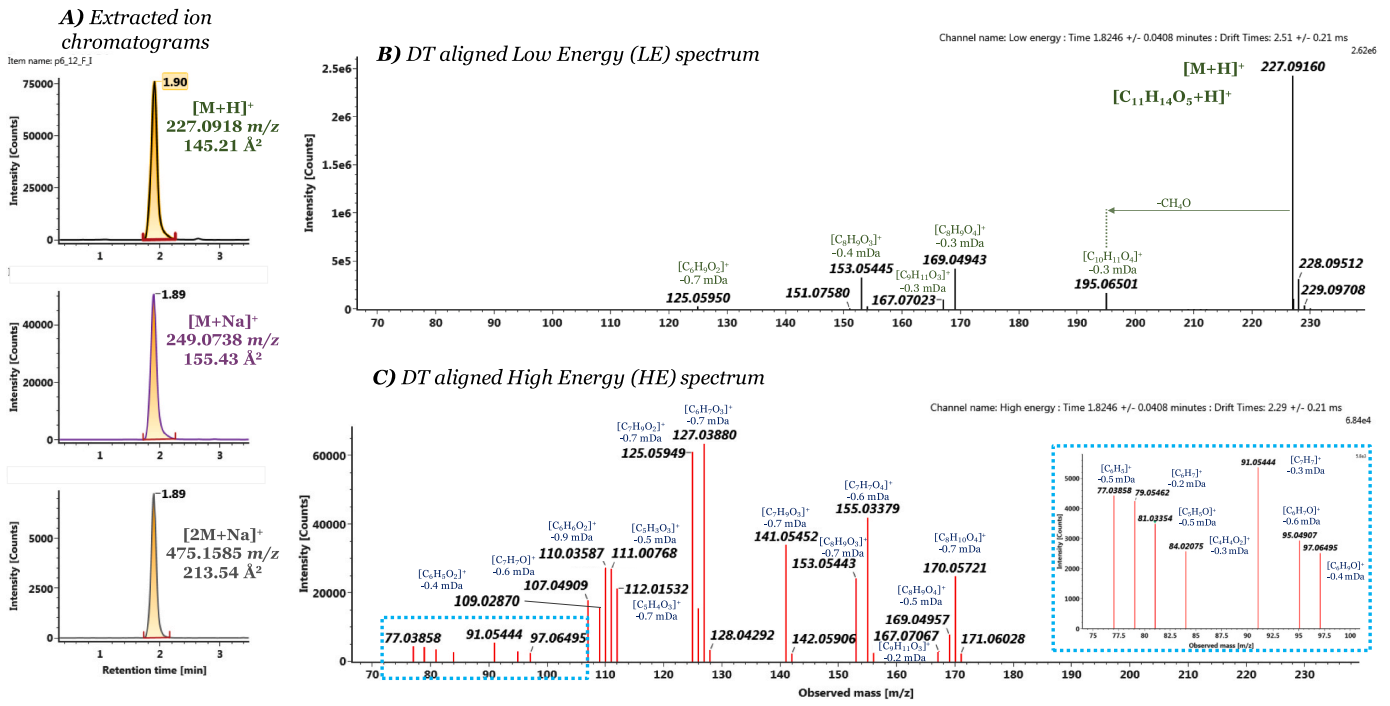

Fig. 5. Marker 6 the chromatograms and HDMS^E spectra: **A**) Extracted ion chromatogram from the LE for the adducts of parent compound along with their experimental *m/z* and CCS, **B**) DT aligned LE spectrum, **C**) DT aligned HE spectrum.

(some of them predicted spectra, other experimental) making difficult to decide on one of them. On other hand, other fragments contributed to identification uncertainty as their presence could not be justified. Fragments *m/z* 77.0386 ($[C_6H_5]^+$, −0.5 mDa error), *m/z* 79.0546 ($[C_6H_7]^+$, −0.2 mDa error) and *m/z* 91.0544 ($[C_7H_7]^+$, −0.3 mDa error, tropylium ion) are known to be present in compounds with a bencilic group (C_6H_5–CH_2-). With this, 4 out of 5 unsaturations attributed to the aforementioned molecular formula would be from a benzene ring, leaving an unsaturation probably as a carbonyl group. The presence of the fragment *m/z* 195.0650 (-CH_4O neutral loss, −0.3 mDa error) in DT aligned LE spectrum could be attributed to some methoxy groups with a methyl (some of the candidates with this group presented this fragment in their spectra). The relatively high polarity of this compound (retention time 1.88 min) would suggest the presence of several alcohol groups that could be attached to the aromatic ring or to an attached alkyl chain. However, this would cause the presence of fragments due to water neutral losses not observed in the fragmentation spectra. In the additional analysis of selected samples in negative ESI mode, no peak was observed at the same retention time, therefore it could not be confirmed the presence of a phenol or acid group (negatively ionisable).

Finally, as an additional tool to try to elucidate marker 6, an in-house Rt and CCS prediction tool developed in our group by Celma et al. was employed [25] (based on previous work in CCS prediction modelling Bijlsma et al., 2017 [19]) for some of the candidate structures (Fig. S5). The relative errors obtained with this prediction tool were below ±4.05% for $[M+H]^+$ and ±5.59% for $[M+Na]^+$, and ±2.32 min for the retention with 95% confidence intervals. It was observed that compounds with many methoxy groups (such as ethyl syringate, 3,4,5-trimethoxyphenyl acetate or 2,4,6-trimethoxyphenyl acetate), showed predicted CCS errors within the accepted limits of the model, but they presented a predicted retention time with a deviation of approximately 4 min, above the accepted error for this parameter. Thus, no tentative identification could be attribute to the candidates selected for the prediction, as none of them get an accepted error for all three parameters predicted. Ultimately, this compound is awaiting further experiments to determine its identity, as HDMS/MS experiments, since due to our group policy for identifications, none of the candidates can be accepted with the current data.

3.4. Putative low-volatile pheromones

As part of the confirmation as a marker of a tentatively identified compound, a bibliographic search was made on its plausibility as a pheromone. This step is especially important to justify the role of the marker in the metabolomic studies carried out. For example, among the possible candidates for marker 2 (finally tentatively identified as urocanic acid) was nicoxamat, an uricosuric drug that in no case would have been given to mice, therefore, it cannot be the identity of the compound, much less a pheromone.

Fig. 6 shows the variation in abundance across weeks of the markers (Table 3) and the comparison between facial and anogenital sampling area. As it can be observed, all the markers were present in the first two weeks of life in samples from facial and anogenital area. An explanation could be that as part of the care that mice dams provide to their pups, there is a constant cleaning by licking. This could cause the distribution of the compounds from one area to the other. In addition, this fact could be also explained if these compounds are released in both areas in aqueous secretions, saliva or tears for the facial area and urine for anogenital area. Alternatively, these compounds are products of the metabolism of keratinocytes, which do not differ between regions of the body. For instance, urocanic acid is a common constituent of the stratum corneum of the epidermis of the skin of mammals with possible photoprotective effect [26]. A simple explanation of why it is enriched in the samples from neonatal pups could be that they are hairless, and this makes the skin outer strata easier to erode even with gentle rubbing of the skin with a cotton swab. Moreover, urocanic acid is a metabolite product of histidine metabolism, particularly abundant in mammalian skin secretion and also present in saliva and urine. Its relevance in chemical communication has been already noticed as an attractant in mammalian skin for parasitic nematodes [27].

Arginine is an amino acid that plays and important role in many metabolic reactions and body functions as cell division, immune functions and protein production among others. It can be found in both urinary excretion and saliva secretion. Due to its high presence in the

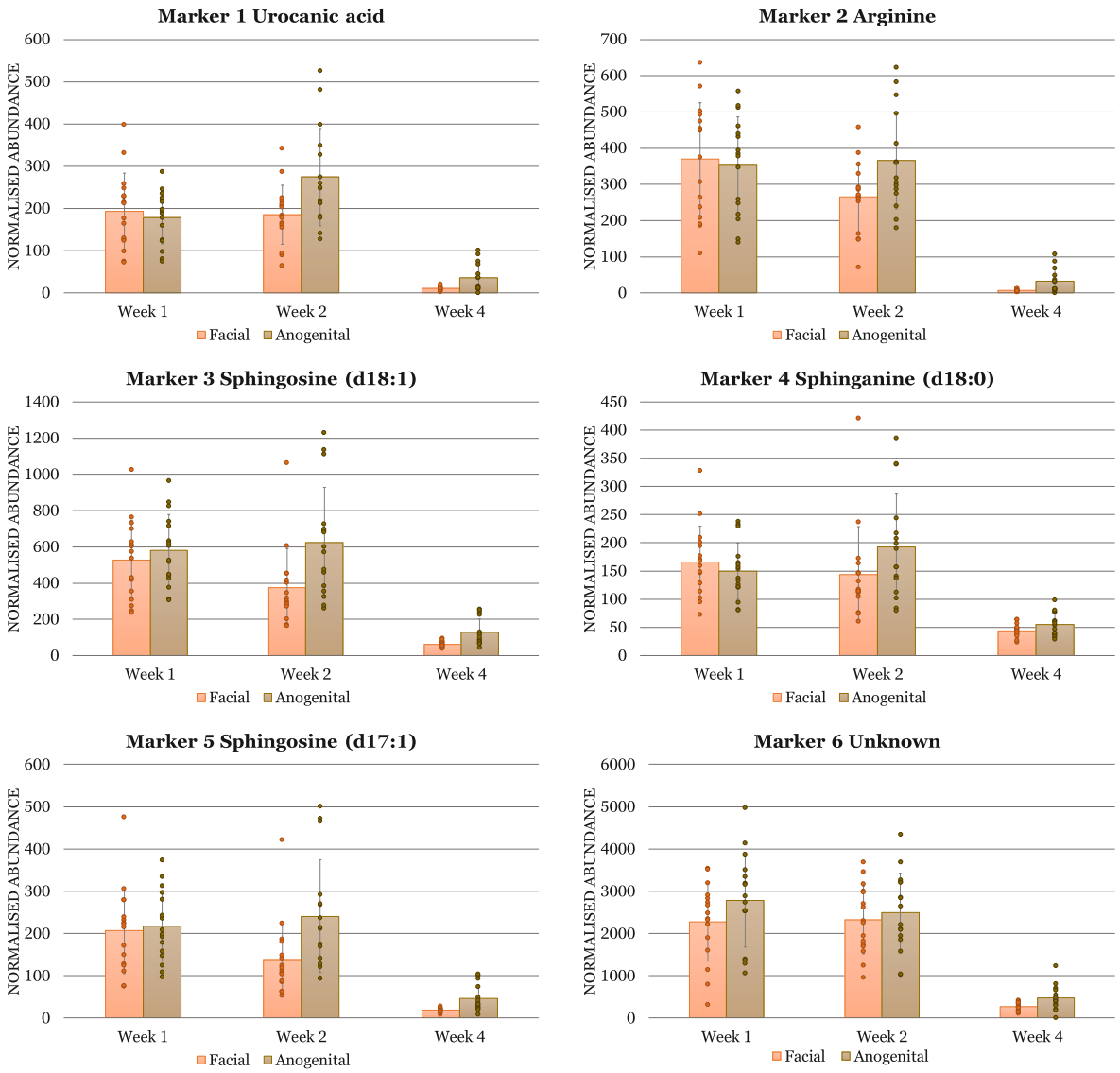

Fig. 6. Comparison of normalized abundance between facial and anogenital areas sampling areas, for the 6 markers. In orange shades the average of normalized abundance obtained from the samples of the same week from facial sampling area (■) and brown shades from anogenital sampling area (■).

body, it is difficult to know if it has a role as pheromone. Although it is widely known that small peptides and bigger proteins can act as such in mice [28], it is unlikely that a simple amino acid can be used for intraspecies communication.

Regarding markers 3, 4 and 5, free-sphingoid bases as sphingosine isomers and sphinganine are employed in different lipids synthesis as ceramides and other sphingolipids that serve as structural and signalling molecules in various cellular events [29]. They are present in all living species ranging from bacteria to humans, and in mammals can be found on the skin (secreted via sebaceous glands), saliva, urine and faeces [30]. Due to their high presence in animals, it is difficult to think that these compounds are pheromones by themselves, since intra-specie communication requires specific molecules that are not easily found in other organisms in the surroundings that could interfere with the communication.

Since an identification for marker 6 has not been reached, it is difficult to determine its plausibility as pheromone. However, compounds with a structure similar to that described in section 3.3 for marker 6 have been reported as pheromones of different organisms (i.e. 3,4-dimethoxycinnamyl alcohol, 4,5-dimethoxyphenol or the isomeric compound 2-hydroxy-3,4,6-trimethoxy-acetophenone found in https://www.pherobase.com/). This demonstrates the potential of marker 6 as a chemical cue and, therefore, its identification will be a target in future research, either by means of the injection of different analytical standards of different candidates or by the use of other analytical techniques.

Therefore, with the exception of marker 6 that awaits identification, the remaining markers seem very common metabolites present in the skin of mammals and/or associated to secretion of exocrine glands (salivary, lacrimal, sebaceous). Although this make them unlikely candidate to pheromones by themselves, when present together in a certain ratio, they may constitute a pheromonal blend [2], a multi-component pheromone characterising the hairless skin of neonatal pups and facilitating maternal care (e.g. licking grooming). This deserves being tested in the near future.

4. Conclusions

Following the first part of the study focused on volatile pheromones, in this work we have successfully applied an untargeted metabolomic approach to discovery of mouse pup low-volatile part of pheromones. Sample collection with swabs allowed the work with alive animals at different stages of their development without interfering in their normal

growths and welfare. The identification of putative low-volatile pheromones involved in the maternal care in mice was possible thanks to the combination of untargeted metabolomics with UHPLC-IMS-HRMS. As in previous work, the differentiating compounds when facing samples from the fourth week of mouse life (time of weaning) against the sample from neonatal mice (first two weeks, receiving maternal care), essentially belonged to the latter. This supports previous studies that suggest the role of chemical communication in maternal care and the hypothesis that this behaviour is induced by compound emitted in the first weeks of life. Five candidates to pup pheromones were tentatively identified, and a sixth compound needs further investigation to give a candidate structure. All of them had a great presence in neonatal pups and shows lower abundance in 4-week youngsters. The introduction of IMS to the well stablished LC-HRMS instruments provided additional structural information that, in combination with CCS, compound and/or spectral databases and CCS predictors models; facilitates the compound identification of most of the compiled markers. Further behavioural research with the tentatively elucidated compounds will be carried out in order to clarify their role in chemical communication for the maternal behaviour induction.

Deontological

These experiments were performed throughout following the European Union Council Directive of June 3rd, 2010 (6106/1/10 REV1). Accordingly, procedures were approved by the Committee of Ethics on Animal Experimentation of the Jaume I University of Castellón where the experiments were performed and, ultimately, by the Valencian *Conselleria d'Agricultura Medi Ambient, Canvi Climàtic i Desenvolupament Rural* (code 2019/VSC/PEA/0049).

Author statement

Leticia Lacalle-Bergeron: Conceptualization, Methodology, Software, Validation, Formal analysis, Investigation, Data curation, Writing - original draft, Writing - review & editing, Visualization, Funding acquisition. **Rafael Goterris-Cerisuelo**: Conceptualization, Methodology, Formal analysis, Investigation, Visualization. **Joaquim Beltrán**: Conceptualization, Methodology, Validation, Investigation, Resources, Writing - review & editing, Visualization, Supervision, Project administration, Funding acquisition. **Juan Vicente Sancho**: Conceptualization, Methodology, Validation, Investigation, Resources, Writing - review & editing, Visualization, Supervision, Project administration, Funding acquisition. **Cinta Navarro-Moreno**: Conceptualization, Investigation, Visualization. **Fernando Martínez-García**: Conceptualization, Methodology, Validation, Investigation, Resources, Writing - review & editing, Visualization, Supervision, Project administration, Funding acquisition. **Tania Portolés**: Conceptualization, Methodology, Validation, Investigation, Resources, Data curation, Writing - review & editing, Visualization, Supervision, Project administration, Funding acquisition.

Declaration of competing interest

The authors declare that they have no known competing financial interests or personal relationships that could have appeared to influence the work reported in this paper.

Data availability

Data will be made available on request.

Acknowledgements

L Lacalle-Bergeron acknowledges the financial support of Universitat Jaume I, Spain for his pre-doctoral grant (UJI 19I001/03). T. Portoles acknowledges Ramon y Cajal Program from the Ministry of Economy and Competitiveness, Spain (RYC-2017-22525) for funding her research. The Research Institute for Pesticides and Water (IUPA) authors acknowledge the financial support of Generalitat Valenciana, as research group of excellence PROMETEO/2019/040 and Universitat Jaume I de Castelló (UJI-B2020-25 and UJI-B2020-37). The Laboratory of Functional Neuroanatomy (Unitat Mixta NeuroFun-UV-UJI) authors acknowledge for financial support of Generalitat Valenciana, as research group of excellence PROMETEO/2017/078, the Spanish Ministry of Science and Innovation (BFU2016-77691-C2; PID2019-107322 GB-C21) and Universitat Jaume I de Castelló (UJI-B2016-45).

Appendix A. Supplementary data

Supplementary data to this article can be found online at https://doi.org/10.1016/j.talanta.2023.124389.

References

[1] P. Karlson, M. Lüscher, 'Pheromones': a new term for a class of biologically active substances, Nature 183 (1959) 55–56, https://doi.org/10.1038/183055a0.
[2] T.D. Wyatt, Pheromones and signature mixtures: defining species-wide signals and variable cues for identity in both invertebrates and vertebrates, J. Comp. Physiol. A. 196 (2010) 685–700, https://doi.org/10.1007/s00359-010-0564-y.
[3] M. Meredith, R.J. O'Connell, Efferent control of stimulus access to the hamster vomeronasal organ, J. Physiol. 286 (1979) 301–316, https://doi.org/10.1113/jphysiol.1979.sp012620.
[4] Y. Isogai, S. Si, L. Pont-Lezica, T. Tan, V. Kapoor, V.N. Murthy, C. Dulac, Molecular organization of vomeronasal chemoreception, Nature 478 (2011) 241–245, https://doi.org/10.1038/nature10437.
[5] T.D. Wyatt, Semiochemicals and social organization, in: Pheromones Anim. Behav., Cambridge University Press, Cambridge, 2014, pp. 126–149, https://doi.org/10.1017/CBO9781139030748.008.
[6] Y. Isogai, Z. Wu, M.I. Love, M.H.-Y. Ahn, D. Bambah-Mukku, V. Hua, K. Farrell, C. Dulac, Multisensory logic of infant-directed aggression by males, Cell 175 (2018) 1827–1841.e17, https://doi.org/10.1016/j.cell.2018.11.032.
[7] T.S. Nakahara, L.M. Cardozo, X. Ibarra-Soria, A.D. Bard, V.M.A. Carvalho, G. Z. Trintinalia, D.W. Logan, F. Papes, Detection of pup odors by non-canonical adult vomeronasal neurons expressing an odorant receptor gene is influenced by sex and parenting status, BMC Biol. 14 (2016) 12, https://doi.org/10.1186/s12915-016-0234-9.
[8] J.G. Vandenbergh, Effects of central and peripheral anosmia on reproduction of female mice, Physiol. Behav. 10 (1973) 257–261, https://doi.org/10.1016/0031-9384(73)90307-7.
[9] Z. Wang, D.R. Storm, Maternal behavior is impaired in female mice lacking type 3 adenylyl cyclase, Neuropsychopharmacology 36 (2011) 772–781, https://doi.org/10.1038/npp.2010.211.
[10] R.S. Bridges, Neurobiology of the Parental Brain, Elsevier, 2008, https://doi.org/10.1016/B978-0-12-374285-8.X0001-7.
[11] L. Lacalle-Bergeron, R. Goterris-Cerisuelo, T. Portolés, J. Beltran, J.V. Sancho, C. Navarro-Moreno, F. Martinez-Garcia, Novel sampling strategy for alive animal volatolome extraction combined with GC-MS based untargeted metabolomics: identifying mouse pup pheromones, Talanta 235 (2021), 122786, https://doi.org/10.1016/j.talanta.2021.122786.
[12] K. Dettmer, P.A. Aronov, B.D. Hammock, Mass spectrometry-based metabolomics, Mass Spectrom. Rev. 26 (2007) 51–78, https://doi.org/10.1002/mas.20108.
[13] L. Lacalle-Bergeron, D. Izquierdo-Sandoval, J.V. Sancho, F.J. López, F. Hernández, T. Portolés, Chromatography hyphenated to high resolution mass spectrometry in untargeted metabolomics for investigation of food (bio)markers, TrAC, Trends Anal. Chem. 135 (2021), 116161, https://doi.org/10.1016/j.trac.2020.116161.
[14] M. Bevilacqua, R. Bro, F. Marini, Å. Rinnan, M.A. Rasmussen, T. Skov, Recent chemometrics advances for foodomics, TrAC, Trends Anal. Chem. 96 (2017) 42–51, https://doi.org/10.1016/j.trac.2017.08.011.
[15] X. Zhang, Q. Li, Z. Xu, J. Dou, Mass spectrometry-based metabolomics in health and medical science: a systematic review, RSC Adv. 10 (2020) 3092–3104, https://doi.org/10.1039/C9RA08985C.
[16] M.-D. Luo, Z.-W. Zhou, Z.-J. Zhu, The application of ion mobility-mass spectrometry in untargeted metabolomics: from separation to identification, J. Anal. Test. 4 (2020) 163–174, https://doi.org/10.1007/s41664-020-00133-0.
[17] C.M. Nichols, J.N. Dodds, B.S. Rose, J.A. Picache, C.B. Morris, S.G. Codreanu, J. C. May, S.D. Sherrod, J.A. McLean, Untargeted molecular discovery in primary metabolism: collision cross section as a molecular descriptor in ion mobility-mass spectrometry, Anal. Chem. 90 (2018) 14484–14492, https://doi.org/10.1021/acs.analchem.8b04322.
[18] C.B. Mollerup, M. Mardal, P.W. Dalsgaard, K. Linnet, L.P. Barron, Prediction of collision cross section and retention time for broad scope screening in gradient reversed-phase liquid chromatography-ion mobility-high resolution accurate mass spectrometry, J. Chromatogr. A 1542 (2018) 82–88, https://doi.org/10.1016/j.chroma.2018.02.025.

[19] L. Bijlsma, R. Bade, A. Celma, L. Mullin, G. Cleland, S. Stead, F. Hernandez, J. V. Sancho, Prediction of collision cross-section values for small molecules: application to pesticide residue analysis, Anal. Chem. 89 (2017) 6583–6589, https://doi.org/10.1021/acs.analchem.7b00741.
[20] B. Worley, R. Powers, Multivariate analysis in metabolomics, Curr. Metabolomics. 1 (2012) 92–107, https://doi.org/10.2174/2213235X130108.
[21] A. Celma, J.V. Sancho, E.L. Schymanski, D. Fabregat-Safont, M. Ibáñez, J. Goshawk, G. Barknowitz, F. Hernández, L. Bijlsma, Improving target and suspect screening high-resolution mass spectrometry workflows in environmental analysis by ion mobility separation, Environ. Sci. Technol. (2020), https://doi.org/10.1021/acs.est.0c05713.
[22] Z. Zhou, J. Tu, X. Xiong, X. Shen, Z.-J. Zhu, LipidCCS: prediction of collision cross-section values for lipids with high precision to support ion mobility–mass spectrometry-based lipidomics, Anal. Chem. 89 (2017) 9559–9566, https://doi.org/10.1021/acs.analchem.7b02625.
[23] V. Hinnenkamp, J. Klein, S.W. Meckelmann, P. Balsaa, T.C. Schmidt, O.J. Schmitz, Comparison of CCS values determined by traveling Wave ion mobility mass spectrometry and drift Tube ion mobility mass spectrometry, Anal. Chem. 90 (2018) 12042–12050, https://doi.org/10.1021/acs.analchem.8b02711.
[24] L. Belova, A. Celma, G. Van Haesendonck, F. Lemière, J.V. Sancho, A. Covaci, A.L. N. van Nuijs, L. Bijlsma, Revealing the differences in collision cross section values of small organic molecules acquired by different instrumental designs and prediction models, Anal. Chim. Acta 1229 (2022), https://doi.org/10.1016/j.aca.2022.340361.
[25] A. Celma, R. Bade, J.V. Sancho, F. Hernandez, M. Humphries, L. Bijlsma, Prediction of retention time and collision cross section (CCS H+ , CCS H– , and CCS Na+) of emerging contaminants using multiple adaptive regression splines, J. Chem. Inf. Model. (2022) 1–16, https://doi.org/10.1021/acs.jcim.2c00847.
[26] N.K. Gibbs, M. Norval, Urocanic acid in the skin: a mixed blessing? J. Invest. Dermatol. 131 (2011) 14–17, https://doi.org/10.1038/jid.2010.276.
[27] D. Safer, M. Brenes, S. Dunipace, G. Schad, Urocanic acid is a major chemoattractant for the skin-penetrating parasitic nematode Strongyloides stercoralis, Proc. Natl. Acad. Sci. USA 104 (2007) 1627–1630, https://doi.org/10.1073/pnas.0610193104.
[28] M.M. Phelan, L. McLean, S.D. Armstrong, J.L. Hurst, R.J. Beynon, L.-Y. Lian, The structure, stability and pheromone binding of the male mouse protein sex pheromone darcin, PLoS One 9 (2014), e108415, https://doi.org/10.1371/journal.pone.0108415.
[29] M.A. Al Sazzad, T. Yasuda, M. Murata, J.P. Slotte, The long-chain sphingoid base of ceramides determines their propensity for lateral segregation, Biophys. J. 112 (2017) 976–983, https://doi.org/10.1016/j.bpj.2017.01.016.
[30] C.L. Fischer, Antimicrobial activity of host-derived lipids, Antibiotics 9 (2020) 75, https://doi.org/10.3390/antibiotics9020075.